Journal of Solid State Electrochemistry
https://doi.org/10.1007/s10008-018-3903-5

ORIGINAL PAPER

Charge transport in carbon electrodes made by electrospray of precursor sol and subsequent carbonization in situ

Madhav P. Chavhan[1] · Pankaj[1] · Somenath Ganguly[1]

Received: 16 September 2016 / Revised: 19 January 2018 / Accepted: 25 January 2018
© Springer-Verlag GmbH Germany, part of Springer Nature 2018

Abstract

As an alternative to binder-based overlay of carbon powder on the current collector, the precursor sol may be carbonized directly on the current collector for the purpose of making supercapacitor electrodes. The disintegration of precursor sol into fine droplets prior to the deposition and subsequent removal of solvent from the deposited gel through lyophilization may enhance the internal surface area and the pore connectivity. This article presents the impedance spectroscopy analysis of such electrodes and reports the resistance to transport of electrolyte ions in such pore network through meaningful equivalent circuits. Neutral, alkaline, and acidic electrolytes were considered in this study. Multiple levels of hierarchy in the pore network are considered here to ascertain the extent of heterogeneity and branching in the pore structure. The electrodes from the binder-based overlay of carbon powder are studied here for comparison. The method of spray coating, followed by in situ carbonization seems to have produced a pore structure, which is less branched. The resistance to access the internal surface is more uniform over the entire domain for such electrodes. The equivalent series resistance was found significantly smaller for these electrodes.

Introduction

The electrochemical double-layer capacitors (EDLCs) are passive electrical energy storage devices with high-power density, good energy density, high reversibility, and longer cycle life. These energy storage devices are used in high power applications including portable electronics, hybrid electric vehicles, smart grids, and storage of solar and wind energy [1–4]. EDLCs differ from the conventional capacitors by the mechanism of charge storage. The charge is stored in the electric double layer at the electrode-electrolyte interface. Activated carbon with high surface area and low costs are widely used as electrode material. Different carbon materials e.g., glassy carbon, carbon in the form of onions, microbeads, cloths, fibers, aerogels, cryogels, xerogels, carbide-derived carbons, and nanotubes [5–19] were used in making EDLC electrodes. The active electrode layer on the current collector is formed through binder-based laying of carbon powder. The making of composite electrode by wetting a fibrous solid with polymeric precursor and subsequent carbonization was also reported [20].

✉ Somenath Ganguly
snganguly@che.iitkgp.ernet.in

[1] Department of Chemical Engineering, Indian Institute of Technology, Kharagpur 721302, India

The capacitance of an EDLC depends on the internal surface area of the electrodes, the pore size distribution, and the resistance, encountered by the ions to access the internal surface. The pore size distribution plays an important role in propagation of electrolyte ions through the pore network. The macropores branch out into the mesopores, through which the ions diffuse into the smallest pores. In order to obtain the maximum charge storage in the double layer, the internal surface area of micro pores needs to be accessed by the electrolyte ions to the fullest extent [8, 19, 21].

In this article, the carbon material for the electrode was obtained from a hydrogel precursor, containing Resorcinol (Re) and Formaldehyde (F). The gel was further processed through freeze drying and carbonization. Important properties of carbon materials from such precursor gels are the high surface area, a tunable nanoporous structure, and a good electrical conductivity [22–26]. Further, a better electrode was developed here by splitting the precursor sol into fine droplets on the current collector, and by retaining the pore structure within the RF gel through use of lyophilization for removal of solvent from the deposited layer.

The pore structure of these electrodes was analyzed by electrochemical impedance spectroscopy (EIS) with aqueous solution of potassium chloride (2 M KCl) as electrolyte. 2 M KOH and 2 M H_2SO_4 solutions were also used as electrolyte in separate experiments for comparison. The EIS is an

Published online: 24 February 2018

effective tool for studying the diffusion of electrolyte ions in a porous electrode [16, 27–30]. Since de Levie's transmission line model [31], various equivalent circuits were proposed to relate the electrochemical impedance at different imposed frequencies to the pore structure of the electrodes. In this article, two equivalent circuits are fitted to the EIS data in order to quantify the ionic resistances at different levels of hierarchy in the pore network. Here, the ladder-type equivalent circuit with three levels in pore hierarchy is considered. Additionally, an equivalent circuit is proposed in this article to study the extent of heterogeneity in the pore structure. In particular, the two parallel sets of RC elements at the lower level of hierarchy in the latter circuit are carefully reviewed to ascertain the extent of heterogeneity in the pore structure. The EIS responses from other electrodes that were derived from the same precursor sol through carbonization in bulk, followed by slurry overlay of carbon powder binder-based carbon overlay are analyzed here for comparison.

Methods

Three types of electrodes were used in this investigation. The first type of electrode was made with activated carbon powder, as purchased. A slurry was prepared with activated charcoal powder (Merck Specialities Pvt. Ltd., Mumbai), Polymethylmethacrylate (Alfa Aesar) as binder, and acetone as solvent. Activated Carbon (AC) and Polymethylmethacrylate (PMMA) were mixed in the ratio of 9:1 (*w*/*w*). An overlay of carbon slurry was applied on a Torey carbon fiber paper (TGP-H-120, with bulk density of 0.45 g/cm^3, electrical resistivity of 80 mΩcm, and thickness of 0.37 mm) using a doctor's blade. This was followed by drying of the coated paper in an oven at 343 K for 5 h. The second type of electrode was also prepared by overlaying carbon slurry. However, the carbon powder for the second type of electrodes was synthesized as part of this study through gelation of resorcinol (Sigma Aldrich) with formaldehyde (Sigma Aldrich) using sodium carbonate (SC) from Sigma Aldrich as the catalyst. The molar ratio of Re to water and Re to F were maintained at 0.018 and 0.5, respectively, in the precursor sol. The molar ratio of Re and SC was maintained constant at 300. The solution was held at 343 K for 24 h to cure the Resorcinol-Formaldehyde (ReF) gel in a glass vial. Next, the gel was lyophilized in a shelf-type freeze drier. The lyophilization procedure involved freezing of gel sample at 243 K, followed by sublimation of solvent through increase in temperature slowly from 243 to 273 K over 12 h under a vacuum of 0.68 Torr. The product was then carbonized in a furnace at 1073 K under a nitrogen gas flow at 100 ml/min. The pressure inside the furnace was maintained at 0.1 Kg/cm^2. The grounded form of carbonized gel was mixed with PMMA binder and acetone to form slurry, as before. The carbon papers were coated with the slurry, and were dried in an oven at 343 K for 5 h. The former type of electrode is referred as AC, and the latter type is referred as ReFC in the following sections. The Brunauer-Emmett-Teller (BET) surface area and pore-size distribution of the carbon powder were estimated from nitrogen adsorption-desorption experiments (Autosorb 1 MP, Quantachrome Instruments, USA).

The third type of electrode was prepared by carbonizing the precursor ReF gel on the carbon paper in situ. The ReF suspension of the same composition, mentioned before was taken out from the oven before the gelation point. The ReF suspension was then flowed into a nozzle of stainless steel through a syringe pump at a rate within the range of 0.5–1.5 mL/h [32]. Electric field was applied across the stainless steel nozzle and the carbon paper. The distance between the tip of the nozzle and the carbon paper was adjusted within the range of 0.7 to 1 cm. A stable cone jet of the ReF suspension disintegrated into fine droplets before impinging on the carbon paper substrate. The coated layer on the carbon paper was cured, lyophilized, and carbonized as per the procedure described before. This type of electrode is referred as EReF in the following sections.

Each set of electrodes was assembled in a plexiglass set-up for electrochemical measurements. The working and the counter electrodes of same mass loading and dimensions were separated by a Whatman®(Grade 1) filter paper. Aqueous solution of KCl at a concentration of 2 M was used as electrolyte. The size of the electrode was taken as 2 cm × 2 cm. The mass of active layer for the ReFC, EReF, and AC electrodes was found

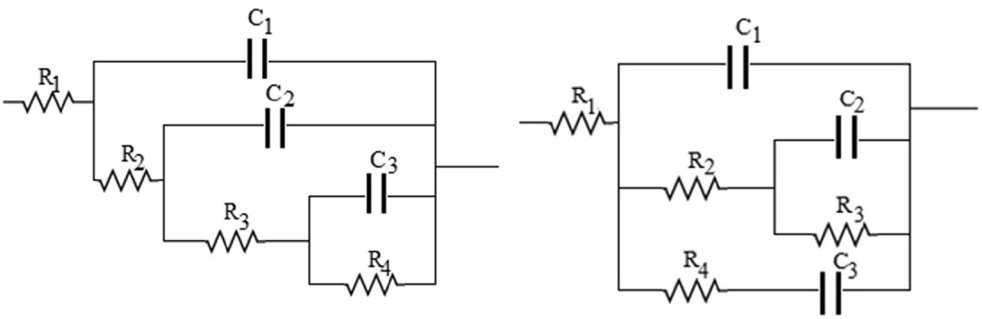

Fig. 1 Schematic diagram of **a** ladder equivalent circuit, and **b** proposed model equivalent circuit

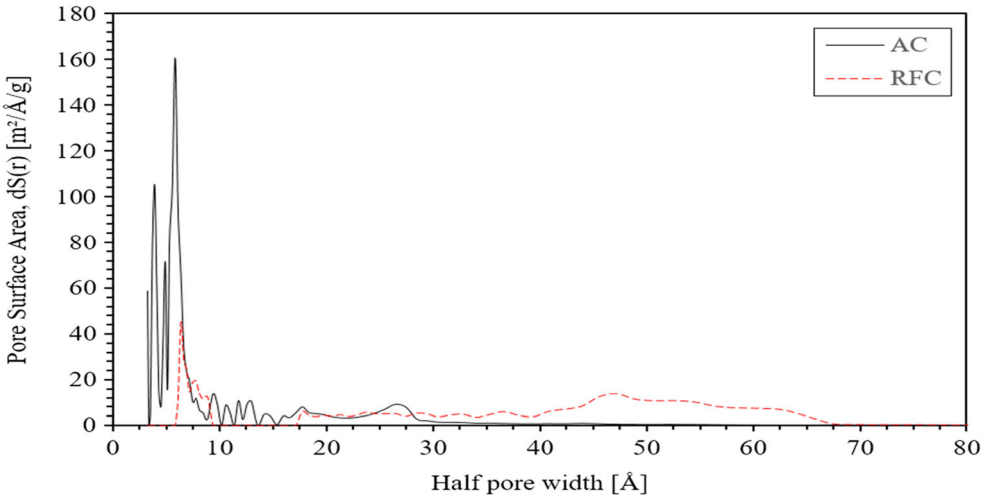

Fig. 2 DFT pore size distribution of carbon powder for ReFC- and AC-type electrodes

as18, 4, and 24 mg, respectively, with the thickness (*t*) of 0.1 mm in each electrode. The electrochemical performance of set of EReF electrodes was also tested with 2 M KOH and 2 M H_2SO_4 solutions. The dimensions for this type of electrodes were taken as 1 cm × 1 cm, with mass of active layer as 0.6 mg.

Electrochemical analyses were performed using Versa Stat 3 (Princeton Applied Research, USA). EIS was conducted over the frequency range of 0.01 Hz to 1 MHz. Cyclic voltammetry and galvanostatic charge-discharge experiments were performed on these sets of electrodes. The experiment was repeated after several charge-discharge cycles to ascertain the irreversible changes in the EReF electrodes. The EIS results were fitted to an equivalent circuit that simulates the hierarchical structure of the pore network and the pore-size

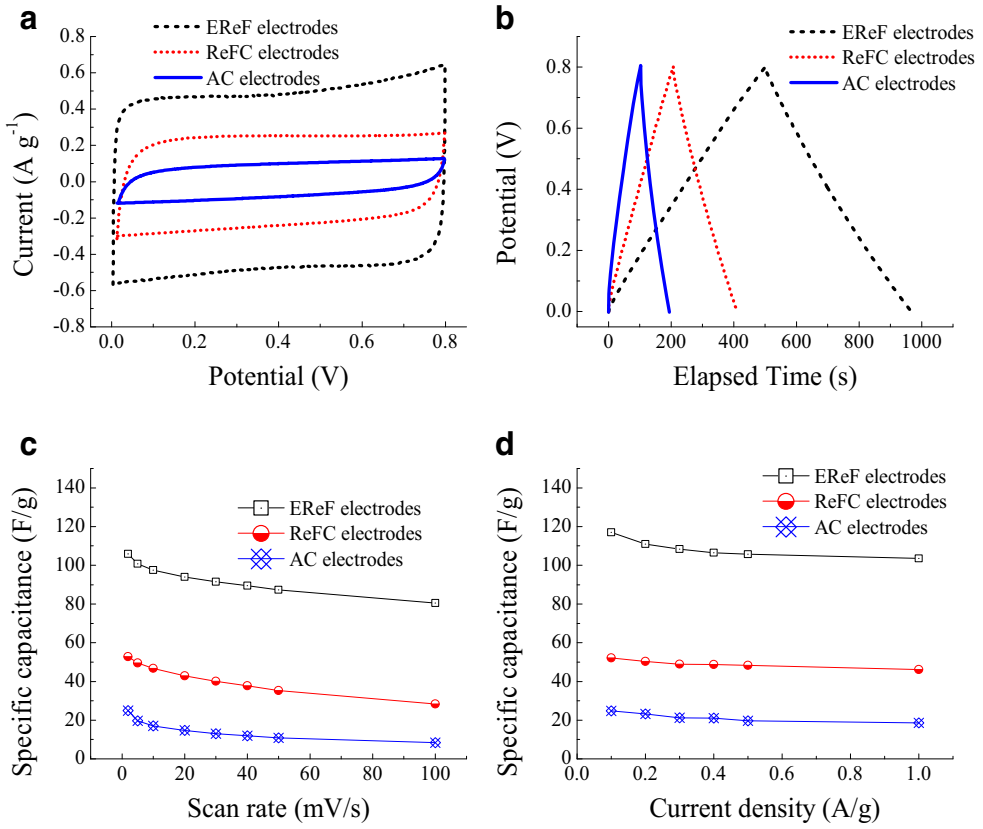

Fig. 3 Electrochemical performance of EReF, ReFC, and AC type of electrodes in 2 M KCl electrolyte. **a** CV at 10 mV/s. **b** CP at 0.1 A/g. **c** Specific capacitance Vs scan rate. **d** Specific capacitance Vs current density

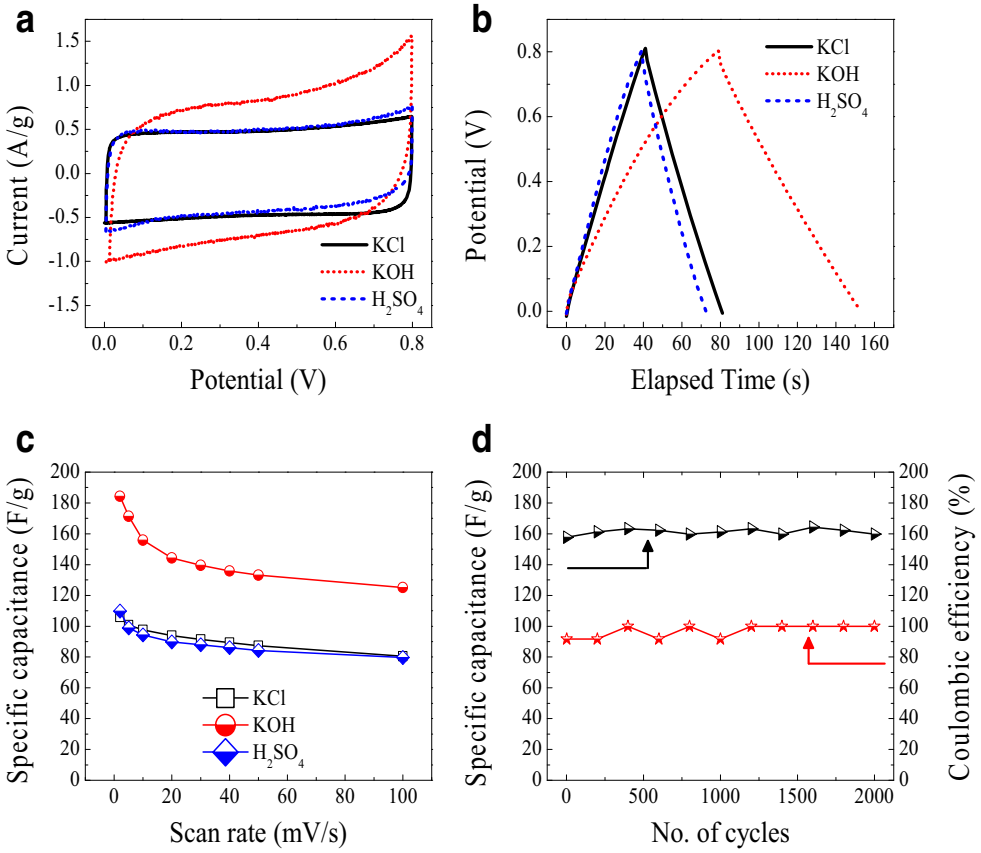

Fig. 4 Electrochemical performance of EReF type of electrodes in KCl, KOH, and H_2SO_4 electrolytes. **a** CV at 10 mV/s. **b** CP at 1 A/g. **c** Specific capacitance Vs scan rate. **d** Cyclic stability in KOH electrolyte at 5 A/g

distribution. The impedance from the resistive and the capacitive elements in the circuit are computed as follows:

$$Z_R = R \tag{1}$$

$$Z_C = \frac{1}{j \times (2\pi\omega C)} \tag{2}$$

Here, R and C are the resistance (in Ohms) and capacitance (in Farads) of the respective circuit elements, ω is the angular frequency in Hz, and $j = \sqrt{-1}$.

The RC elements were regressed to match the overall impedance of the circuit with the impedance, derived from the EIS data. For the purpose of error minimization, the objective function, f is defined in Eq. 3. The

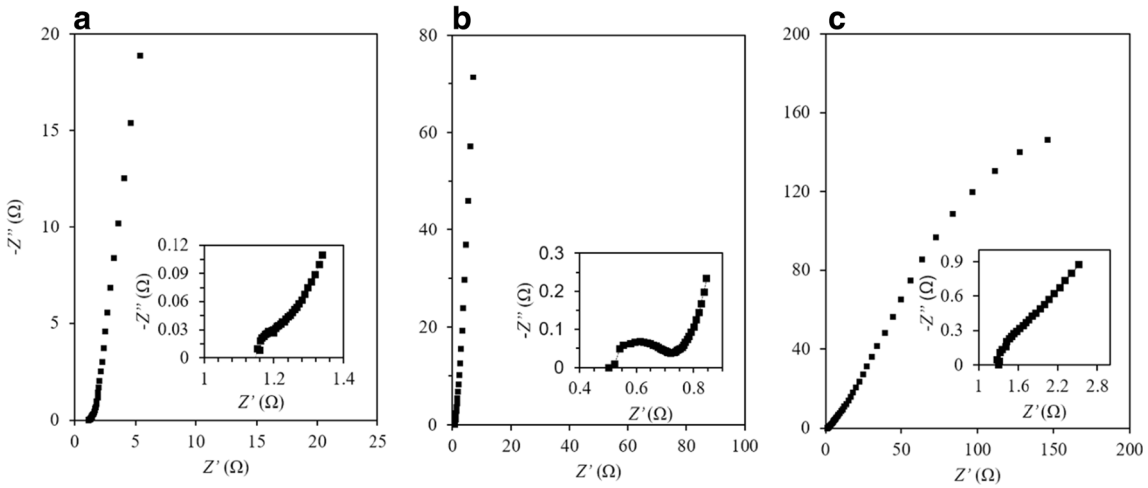

Fig. 5 Nyquist spectra for **a** ReFC-, **b** EReF-, and **c** AC-type electrodes

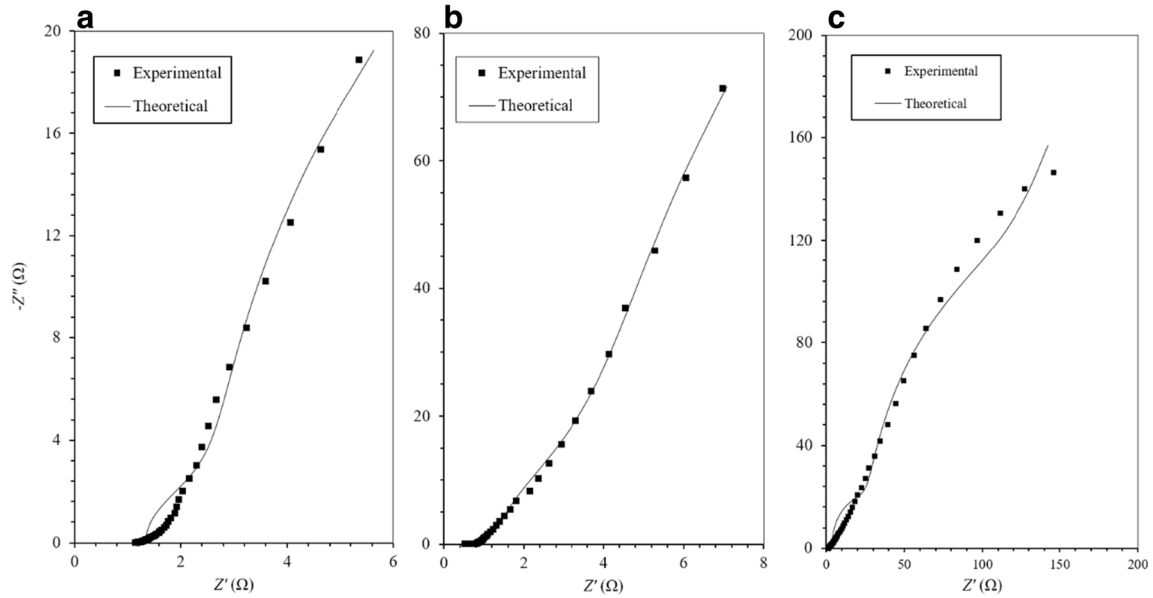

Fig. 6 Impedance spectra fitted with ladder model for **a** ReFC-, **b** EReF-, and **c** AC-type electrodes

simplex algorithm of error minimization was implemented using Matlab R2013b from Mathworks Inc. The goodness of fit is represented here by the Chi^2 value (χ^2) as defined below.

$$f = \sum\left((Z\text{theo}-Z\text{exp})^2\right) \tag{3}$$

$$\chi^2 = \sum \frac{(Ztheo_{\text{re}} - Zexp_{\text{re}})^2 + (Ztheo_{\text{im}} - Zexp_{\text{im}})^2}{\sigma^2} \tag{4}$$

$$\sigma^2 = (Zexp_{\text{re}} + Ztheo_{\text{re}})^2 \tag{5}$$

Here, $Z\text{exp}_{\text{re}}$ and $Z\text{theo}_{\text{re}}$are the real components of overall impedance from the EIS data and the equivalent circuit model, respectively. $Z\text{exp}_{\text{im}}$ and $Z\text{theo}_{\text{im}}$ are the respective imaginary counterparts. *Z*exp and *Z*theo are overall impedance from EIS data and the equivalent circuit model, respectively. Two equivalent circuits are considered (Fig. 1) in this investigation. The initial guess was varied systematically over the entire search space to ensure that the converged values of *RC* elements lead to the global minimum.

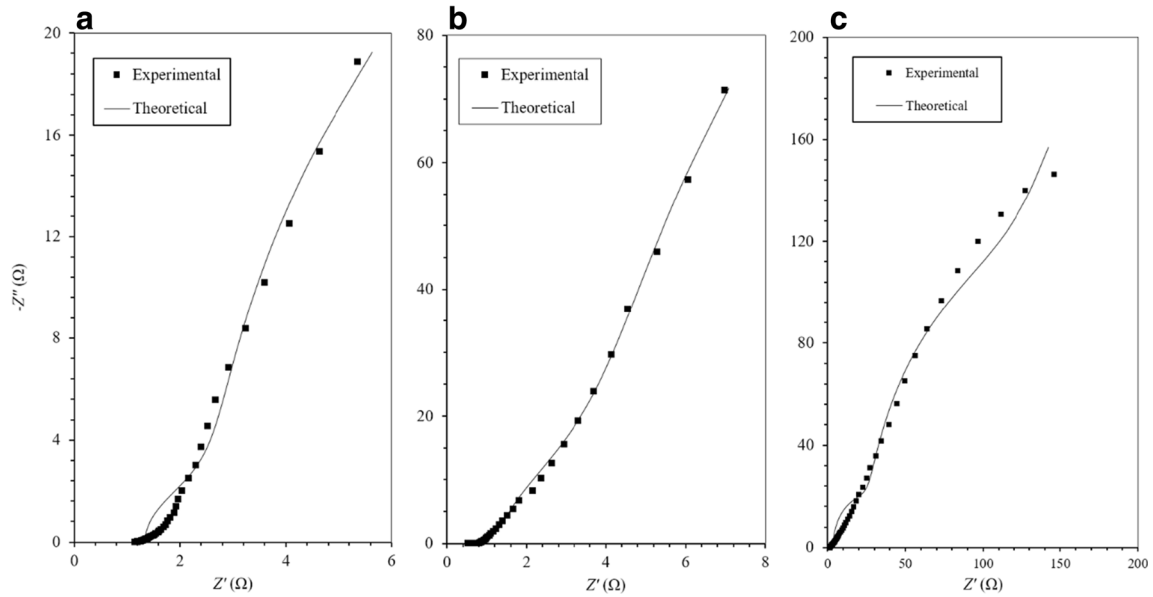

Fig. 7 Impedance spectra fitted with proposed model for **a** ReFC-, B) EReF-, and (C) AC-type electrodes

Table 1 The regressed values of RC elements (ladder model)

Electrode type	R_1 (Ω)	C_1 (F)	R_2(Ω)	C_2 (F)	R_3(Ω)	C_3 (F)	R_4(Ω)	Chi^2
ReFC	1.20	1.9×10^{-2}	0.21	0.205	0.99	0.42	16.7	6.4×10^{-4}
EReF	0.60	4.1×10^{-4}	0.17	0.175	3.99	0.07	76.1	3.9×10^{-3}
AC	3.55	7.8×10^{-3}	39.21	0.033	218.69	0.11	1949	2.0×10^{-2}

Results and discussions

The carbon material is known for a porosity at multiple scales. Figure 2 compares the DFT pore-size distribution of two types of carbon powders, used in this study. These distributions were computed from the nitrogen adsorption studies in a BET apparatus. The presence of meso and microporosity is evident in both the samples. The BET surface area for the AC and ReFC powders were found to be 900.15 m^2/g and 944.02 m^2/g. Understandably, most of the internal surface is held in micropores, and the access to these micropores is provided by the mesopore network. From our experience, the presence of binder reduced the BET surface area to half of the original value.

The results from the cyclic voltammetry (CV) and the chronopotentiometry (CP) are reported in Fig. 3. The rectangular and triangular profiles in CV and CP plot, respectively, show behavior of ideal double-layer charge storage. The specific capacitance values are reported here at varied scan rate and current density, respectively. The specific capacitance was found highest for the EReF type of electrodes, and the capacitance value reached up to 120 F/g.

The above observations with neutral electrolyte were further analyzed and compared by repeating the electrochemical tests with alkaline and acidic electrolytes. Figure 4 presents the CV and CP plots for the neutral, alkaline, and acidic electrolytes, respectively, obtained with EReF electrodes. In case of KOH electrolyte, the distortion in rectangular shape of CV plot occurs at the higher voltage. Understandably, the OH^- ions form a reactive interaction with the carbon surface easily, and at a lower voltage, compared to other electrolytes. The specific capacitance was found higher with KOH as electrolyte. The capacitance and the Coulombic efficiency with KOH electrolyte are retained to the respective original values of 159.68 F/g (at 5 A/g) and 100% after 2000 charge-discharge cycles.

The Nyquist spectra are plotted in Fig. 5 for different types of electrodes. The equivalent series resistance (ESR) that represents the internal resistance of the capacitor may be estimated from the intercept on real impedance axis at high frequency. The ESR was found least with the electrodes that were electrospray-coated, and subsequently carbonized in situ. This ESR value is less than half of the ESR values, reported for other electrodes. The *ESR* for EReF electrodes may further be reduced by suitable activation method.

The ESR values show the lowest ESR for EReF-type electrode, and the highest for activated carbon-overlay (AC)-type electrodes. That is, the reduction of ESR is consistent with the superior performance of the EReF electrodes. Also, the performance of ReFC-type electrodes demonstrates the effectiveness of resorcinol-formaldehyde gel as a carbon precursor. This observation is consistent with the BET data, reported in the earlier paragraph. The AC electrodes are made of activated charcoal powder, as purchased with BET surface area of 900.15 m^2/g. The use of binder will reduce the accessible surface area to half of original value. The ReFC electrodes are made of not-activated carbon powder, obtained from RF precursor sol. The BET surface area of such carbon powder was found to be 944.02 m^2/g, which gets reduced further due to the presence of binder. EReF electrodes are based on this same not-activated carbon powder. However, in EReF electrodes, the RF sol was split into small droplets, when placed on carbon collector prior to the carbonization of sol. Further, the use of binder could be avoided that helped retaining the access to internal surface area.

The Nyquist spectra are further analyzed using two equivalent circuits, described in Fig. 1. One is the conventional ladder circuit. This circuit represents a branched network of pores with three levels of hierarchy. An example of such network may be macro-meso-micro pore composite, where the meso-pores originate from the wall of the macropore, and finally branch into the micropores. The charge transfer resistance to access the pores in next level of hierarchy, the double-layer capacitance at each level of hierarchy, and the non-ideality of the capacitance at the lowest hierarchy (leakage resistance) are estimated by fitting the data to the equivalent circuit model. Other than the ladder model, a new circuit is proposed in this article (Fig. 1b). Here, instead of a single set of pore resistance and double-layer capacitance at the lower

Table 2 The regressed values of RC elements (proposed model)

Electrode type	R_1 (Ω)	C_1 (F)	R_2 (Ω)	C_2 (F)	R_3 (Ω)	R_4 (Ω)	C_3 (F)	Chi^2
ReFC	1.20	0.019	1.04	0.48	16.90	0.27	0.132	6.4×10^{-4}
EReF	0.59	3×10^{-4}	0.20	0.11	81.96	4.15	0.072	3.8×10^{-3}
AC	4.61	8.7×10^{-3}	208.75	0.104	4.86×10^2	48.56	0.021	2.4×10^{-2}

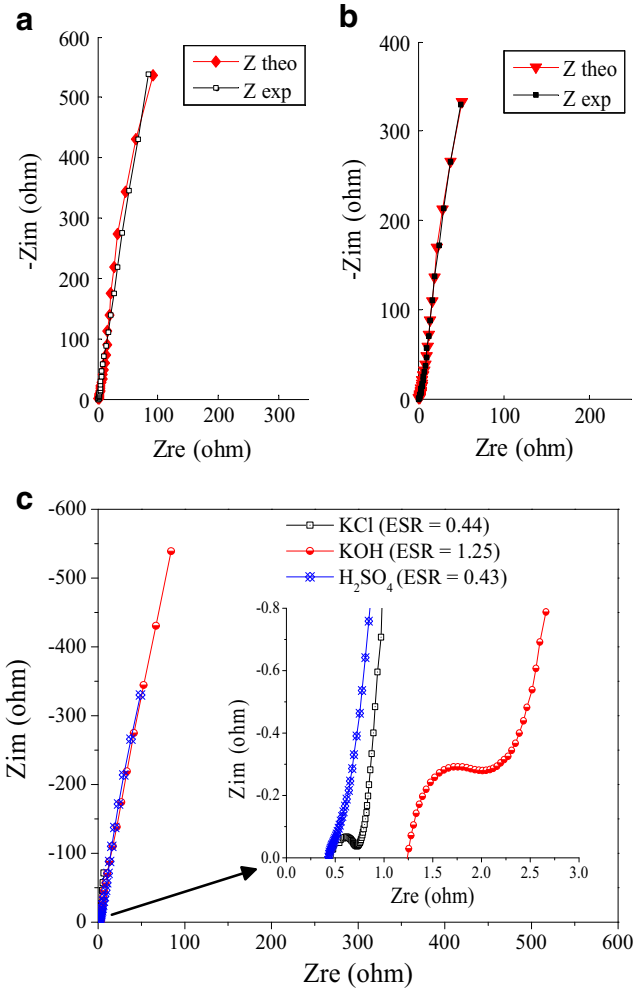

Fig. 8 Impedance spectra fitted with proposed model for EReF-type electrodes **a** KOH, **b** H_2SO_4, and **c** comparison of Nyquist plot for three electrolytes

level of hierarchy, two different sets of RC elements are considered. The use of this equivalent circuit enables an assessment of the non-uniformity of the pores.

Figures 6 and 7 present the match of EIS data with the output from the two equivalent circuit models. From these two figures, both the models appeared to have fitted the experimental EIS data with similar accuracy. The fit was better for EReF-type electrode, compared to the match for slurry coated electrodes. Tables 1 and 2 present the fitted values of the circuit parameters. From the fit of the ladder model, the resistance to access the first level of pore hierarchy was found lowest for EReF-type electrodes. Understandably, this resistance accounts for the cumulative effect of bulk electrolyte resistance, interfacial resistance, and contact resistances (both intra-particle, and between the particle and the current collector). As such, this resistance is significantly smaller for the carbon sample, derived from ReF gel. Further, the resistance to access the lowest level of pore hierarchy in the ladder model was significantly higher for EReF-type electrodes. This is in spite of higher overall capacitance, shown by the EReF-type electrodes, leading to a hypothesis that the pores in EReF-type electrodes did not possess much of a hierarchy. The pores were less branched, and were more homogeneous, as compared to the pores in the other electrodes. The C_2 values, when normalized by the mass of active layer are 11.39, 43.75, and 1.37 F/g, respectively, for ReF-, EReF-, and AC-type electrodes. The specific capacitance values of the corresponding electrodes from CV measurements at scan rate of 100 mV/s are in the order of 30, 80, and 10 F/g, respectively. The C_2 values are essentially a major component of equivalent circuit, contributing to the double-layer capacitance. The estimates of C_2 are based on impedance measurements over a very wide range of frequency. However, the relative magnitude of C_2 values from the model fitting for different electrodes are found consistent with the capacitance values from other measurements.

The trends from the ladder-type equivalent circuit are well supported by the other model of pore network, considered in this article. In the other equivalent circuit, a parallel RC branch is introduced at the second level of hierarchy to investigate further the extent of heterogeneity in the pore structure. The comparisons of R_2 with R_4 and of C_2 with C_3 for the ReFC- and EReF-type electrodes show a clear distinction between the two sets of pores in EReF electrodes. The EReF pores with resistance R_2 are easily penetrable, as the value of R_2 is quite smaller than the value of R_4. Also, the same set of easily penetrable pores in EReF electrodes provides higher double-layer capacitance (C_2). The other set of EReF pores with resistance R_4 possesses much higher resistance (~ 24 times the former value), and smaller double-layer capacitance (C_3). In other words, an attempt to classify the pores into two sets ended up in one set that is impenetrable and with low internal surface area, compared to the other set of pores. The double-layer charge is stored primarily in the former set of pores. The difference between the two parallel RC branches are not pronounced in case of ReFC-type electrodes, where both set of pores are holding double layer for charge storage by varying extents. Thus, the

Table 3 The regressed values of RC elements (proposed model) with three electrolytes KCl, KOH, and H_2SO_4 for EReF type of electrodes

Electrolyte (2 M)	R_1 (Ω)	C_1 (F)	R_2 (Ω)	C_2 (F)	R_3 (Ω)	R_4 (Ω)	C_3 (F)	Chi^2
KCl	0.59	3×10^{-4}	0.20	0.11	81.96	4.15	0.072	3.8×10^{-3}
KOH	1.56	1.26×10^{-3}	1.66	1.99×10^{-2}	3843	169.32	0.008	3.03×10^{-2}
H_2SO_4	0.56	2.31×10^{-2}	15.6	1.28×10^{-2}	2911	191.36	0.011	6.38×10^{-2}

existence of a homogeneous and less branched set of pores in EReF-type electrodes is indicated from this study.

Figure 8 presents the match of EIS data with the output from the proposed equivalent circuit using KOH and H_2SO_4 electrolytes. A comparison of the model parameters is drawn in Table 3. The ESR for the three electrolytes was found to be 0.44, 1.25, and 0.43 Ω, respectively (Fig. 8c. The value of R_2 (Table 3) increased significantly with H_2SO_4 as electrolyte, suggesting the hindrance to penetration of bulky SO_4^{2-} into smaller pores. The observations on penetrability of the two sets of pores (comparison of R_2 and R_4, reported in the previous paragraph) still hold for alkaline and acidic electrolytes, substantiating the existence of homogeneous pores in EReF electrodes.

Conclusions

The resistances, encountered by the electrolyte ion in a novel electrode structure were analyzed in this article. The novel electrode was made by leveraging (*i*) the electrospray process to split the precursor sol on the current collector, (*ii*) lyophilization process to retain the pore space within the gel network at the time of solvent removal, and (*iii*) in situ carbonization process. Here, the carbonization of precursor sol in atomized droplets can provide uniform pore structure. The making of novel electrode did not involve any use of binder. Accordingly, any hindrance in accessing the internal surface due to the presence of binder could be avoided. The transport of electrolyte ions through such electrode was analyzed from the impedance spectroscopy data. For comparison, the slurry coated electrodes with carbon powder, made from the precursor sol of same composition was studied. High specific capacitance of the novel electrode was found consistent with the low value of ESR. Two equivalent circuits were employed to study the extent of branching and heterogeneity in the pore structure. From this modeling exercise, the pores in the novel electrode appeared to be more homogeneous. The reduced branching and hierarchies in the pore network seemed to have contributed to the specific capacitance of the novel electrode. The observations are applicable generally to neutral, acidic, and alkaline electrolytes. The specific capacitance of 160 F/g at current density of 5 A/g was observed with KOH electrolyte in these electrodes. This capacitance at a coulombic efficiency of 100% was retained after 2000 charge-discharge cycles. Further improvement in performance of this electrode is anticipated through tuning the spray process and activation of the final product.

Therefore, in any carbon gel, a meso and micropore network is invariably present, and serves the purpose of double-layer formation here. The EReF electrodes seem to have a favorable hierarchy, which is evident from the electrochemical studies (CV and CP analysis) with the three types of electrolytes. The trends are consistent for this novel electrode at varying current densities and after several charge-discharge cycles. Further, the EIS studies revealed a lower ESR value for this type of electrode, compared to the traditional ones. An equivalent circuit model is proposed here to test the homogeneity of pore resistance across the active layer, based on the EIS data. The analysis suggests more uniform pores in the new type of electrode.

References

1. Sarangapani S, Tilak BV, Chen CP (1996) Materials for electrochemical capacitors: theoretical and experimental constraints. J Electrochem Soc 143:3791–3799
2. Simon P, Gogotsi Y (2008) Materials for electrochemical capacitors. Nature Mat 7(11):845–854. https://doi.org/10.1038/nmat2297
3. Miller JR, Simon P (2008) Electrochemical capacitors for energy management. Science 321(5889):651–652. https://doi.org/10.1126/science.1158736
4. Simon P, Gogotsi Y, Dunn B (2014) Where do batteries end and supercapacitors begin? Science 343:1210–1211
5. Conway BE (1999) Electrochemical supercapacitors: scientific fundamentals and technological applications. Kluwer Academic/Plenum Press, New York. https://doi.org/10.1007/978-1-4757-3058-6
6. Kötz R, Carlen M (2000) Principles and applications of electrochemical capacitors. Electrochim Acta 45(15-16):2483–2498. https://doi.org/10.1016/S0013-4686(00)00354-6
7. Burke A (2000) Ultracapacitors: why, how, and where is the technology. J Power Sources 91(1):37–50. https://doi.org/10.1016/S0378-7753(00)00485-7
8. Qu D, Shi H (1998) Studies of activated carbons used in double-layer capacitors. J Power Sources 74(1):99–107. https://doi.org/10.1016/S0378-7753(98)00038-X
9. Qu D (2001) The ac impedance studies for porous MnO_2 cathode by means of modified transmission line model. J Power Sources 102(1-2):270–276. https://doi.org/10.1016/S0378-7753(01)00810-2
10. Frackowiak E, Béguin F (2001) Carbon materials for the electrochemical storage of energy in capacitors. Carbon 39(6):937–950. https://doi.org/10.1016/S0008-6223(00)00183-4
11. Frackowiak E, Meteneir K, BertagnaV BF (2000) Supercapacitor electrodes from multiwalled carbon nanotubes. Appl Phys Lett 77:2421–2423
12. Shi H (1996) Activated carbons and double layer capacitance. Electrochim Acta 41(10):1633–1639. https://doi.org/10.1016/0013-4686(95)00416-5
13. Gamby J, Taberna PL, Simon P, Fauvarque JF, Chesneau M (2001) Studies and characterisations of various activated carbons used for carbon/carbon supercapacitors. J Power Sources 101:109–116
14. Lin C, Ritter JA, Popov BN (1999) Correlation of double-layer capacitance with the pore structure of sol-gel derived carbon xerogels. J Electrochem Soc 146:3639–3643
15. Song HK, Hwang HY, Lee KH, Dao LH (2000) The effect of pore size distribution on the frequency dispersion of porous electrodes. Electrochim Acta 45(14):2241–2257. https://doi.org/10.1016/S0013-4686(99)00436-3
16. Taberna PL, Simon P, Fauvarque JF (2003) Electrochemical characteristics and impedance spectroscopy studies of carbon-carbon supercapacitors. J Electrochem Soc 150:A292–A300

17. Meyer ST, Pekala RW, Kaschmitter JL (1993) The Aerocapacitor: an electrochemical double-layer energy-storage device. J Electochem Soc 140:446–451
18. Niu CM, Sichel EK, Hoch R, Moy D, Tennet H (1997) High power electrochemical capacitors based on carbon nanotubes electrodes. Appl Phys Lett 70:1480–1482
19. Salitra G, Soffer A, Eliad L, Cohen Y, Aurbach D (2000) Carbon electrodes for double-layer capacitors I. Relations between ion and pore dimensions. J Electrochem Soc 147:2486–2493
20. Bruno M M, Cotella N G, Miras M C, Barbero C A (2005) Porous carbon–carbon composite replicated from a natural fibre. Chem Commun 0:5896–5898, 47, DOI: https://doi.org/10.1039/b511771b
21. Chimola J, Yushin G, Gogotsi Y, Portet C, Simon P, Taberna PL (2006) Anomalous increase in carbon capacitance at pore size less than 1 nanometer. Science 313(5794):1760–1763. https://doi.org/10.1126/science.1132195
22. Tamon H, Ishizaka H, Yamamoto T, Suzuki T (2000) Influence of freeze-drying conditions on the mesoporosity of organic gels as carbon precursors. Carbon38:1099–1105
23. Wu D, Fu R, Zhang S, Dresselhaus MS (2004) Dresselhaus G (2004) preparation of low-density aerogels by ambient pressure drying. Carbon 42(10):2033–2039. https://doi.org/10.1016/j.carbon.2004.04.003
24. Li J, Wang X, Wang Y, Huang Q, Dai C, Gamboa S, Sebastian PJ (2008) Structure and electrochemical properties of carbon aerogels synthesized at ambient temperatures as supercapacitors. J Non-Cryst Solids 354:19–24
25. Pröbstle H, Wiener M, Fricke J (2003) Carbon aerogels for electrochemical double layer capacitors. J Porous Mater 10:213–222
26. Kim J, Hwang SW, Hyun SH (2005) Preparation of carbon aerogel electrodes for supercapacitors and their electrochemical characteristics. J Mater Sci 40:725–731
27. Candy JP, Fouilloux P, Keddam M, Takenouti H (1981) The characterization of porous electrodes by impedance measurements. ElectrochimActa 26(8):1029–1034. https://doi.org/10.1016/0013-4686(81)85072-4
28. Keiser H, Beccu KD, Gutjahr MA (1976) Abschätzung der porenstruktur poröser elektroden aus impedanzmessungen. Electrochim Acta 21:539–543
29. Srinivasan V, Weidner J (1999) Mathematical modeling of electrochemical capacitors. J Electochem Soc 146(5):1650–1658. https://doi.org/10.1149/1.1391821
30. Lufrano F, Staiti P, Minutoli M (2003) Evaluation of nafion based double layer capacitors by electrochemical impedance spectroscopy. J Power Sources 124:314–320
31. Levie RD (1964) On porous electrodes in electrolyte solution-IV. Electrochim Acta 9(9):1231–1245. https://doi.org/10.1016/0013-4686(64)85015-5
32. Ganguly S, Chavhan MP (2016) An improved carbon electrode for electric double layer capacitor devices and a method of fabricating said improved carbon electrode Indian Patent:201631000006